MAGNETIC RESONANCE IN CHEMISTRY
Magn. Reson. Chem. **36**, 732–740 (1998)

Pseudorotation of the sugar moiety in pyrimidine nucleosides occurs on the same time-scale as the overall tumbling: ^{2}H NMR relaxation time study

Janez Plavec,[1]* Peter Roselt,[2] Andras Földesi[2] and Jyoti Chattopadhyaya[2]*

[1] National Institute of Chemistry, Hajdrihova 19, SI-1115 Ljubljana, Slovenia
[2] Department of Bioorganic Chemistry, Box 581, Biomedical Centre, University of Uppsala, S-751 23 Uppsala, Sweden

Received 11 February 1998; revised 11 May 1998; accepted 12 May 1998

ABSTRACT: The molecular motions of specifically deuterated thymidines **1**–**5a** and two C-3-deuterated allofuranoses **6** and **7** were studied through temperature-dependent ^{2}H and ^{13}C relaxation times. Deuterium relaxation times in **1**–**5a** were found in the range 20–270 ms between 278 and 358 K, respectively. Interpretation of deuterium T_1 relaxation time, which is dominated by quadrupole mechanism, gave the effective rotational correlation time (τ_{eff}) in the range from 62.5 ps in 2′,6-diDT (**4**) to 117.5 ps in 6-DT (**3**) at 278 K. The τ_{eff} values are reduced to 9.3 ps in 2′,6-diDT (**4**) to 16 ps in 6-DT (**3**) at 358 K. The τ_{eff} values for **6** and **7** are 93.9 and 100.4 ps, respectively, at 278 K, and are reduced to 19.8 and 22.6 ps, respectively, at 328 K. A deuterium quadrupole coupling constant (e^2qQ/h) of 167 kHz was calculated from ^{2}H and ^{13}C relaxation times in 2′-DT (**1**). Arrhenius-type analysis of temperature-dependent deuterium T_1 relaxation times in **1**–**7** gave apparent activation energies in the range 20–23 ($\pm$0.9) kJ mol^{-1}. Deuterium in anh-6-DT (**5a**) served as a reference for the evaluation of the activation energy of the overall molecular reorientation in the conformationally free counterparts **1**–**4** due to the fact that rotation across χ and N$\rightleftharpoons$S repuckering are prevented by its structure. The comparison of the apparent activation energies from the conformationally free nucleosides **1**–**4** with those from the constrained analogue **5a** and abasic sugars **6** and **7** suggests that their internal local motions are heavily coupled with the overall molecular reorientation, thus preventing the estimation of the pseudorotation energy barrier. © 1998 John Wiley & Sons, Ltd.

KEYWORDS: NMR; ^{2}H NMR; ^{13}C NMR; relaxation; pseudorotation; conformation; deuterated nucleoside

INTRODUCTION

Natural nucleosides consist of a heterocyclic nucleobase and a D-ribo or 2′-deoxy-D-ribofuranose moiety which are covalently linked by a heteroatom of the heterocycle to the C-1′ of the sugar (i.e. anomeric centre) in a β-configuration.[1] From numerous x-ray studies it is known that ribofuranose moieties in natural nucleosides adopt predominantly two distinct north (N) and south (S) conformational families.[1,2] From a large collection of NMR data in solution it is well established that the sugar moieties of nucleos(t)ides are involved in a two-state conformational equilibrium between N and S conformations which are dynamically interconverting in solution. The hypothesis of the two-state model in solution has been experimentally evidenced by the NMR observations of two distinctly identifiable and dynamically interconverting N and S conformations of the sugar moieties in oligonucleotides as in B$\rightleftharpoons$Z DNA,[3a,b] A$\rightleftharpoons$Z RNA[3c,d] or A-form$\rightleftharpoons$B-form lariat RNA[3e,f] transitions. Assuming that the two-state model is valid, we have shown[4] that the conformation of the sugar in nucleos(t)ides is driven by the balance of stereoelectronic and steric effects. We found[4] that the strength of the stereoelectronic forces is dictated by protonated/neutral/deprotonated state of the nucleobase, which is in turn dictated by the pD of the medium. For β-D-2′,3′-dideoxy-,[4u] β-D-2-deoxy-,[4n] β-D-ribo-*N*-nucleosides,[4n] β-D-ribo-*C*-nucleosides[4r] and α-D-2′,3′-dideoxy-[4u] and α-D-2′-deoxyribo-*N*-nucleosides[4u] the pDs at the inflection points of the sigmoidal plots of pD-dependent ΔG° of N$\rightleftharpoons$S equilibria correspond to the pK_as of the nucleobases. This confirmed that the pentofuranose moiety in nucleos(t)ides is indeed engaged in a two-state equilibrium in D_2O solution.

Fast transitions between N and S states occur in solution on a nanosecond time-scale at ambient temperature, which results in the time-averaged NMR coupling constants and chemical shifts of sugar moieties in nucleosides.[1–4] The N$\rightleftharpoons$S pseudorotational equilibrium of the sugar moiety is in solution energetically (ΔG°) controlled by various competing stereoelectronic effects (ΔH°) which are determined by the stereochemical position of the heterocyclic base, CH_2OH group and

* Correspondence to: J. Plavec, National Institute of Chemistry, Hajdrihova 19, SI-1115 Ljubljana, Slovenia or J. Chattopadhyaya, Department of Bioorganic Chemistry, Box 581, Biomedical Centre, University of Uppsala, S-751 23 Uppsala, Sweden.
E-mail: janez.plavec@ki.si
Contract/grant sponsor: Swedish Natural Science Research (NFR) Council.
Contract/grant sponsor: Swedish Technical Research Council (TFR).
Contract/grant sponsor: Ministry of Science and Technology of the Republic of Slovenia.

 CCC 0749-1581/98/100732–09 $17.50

other substituents on the α- or β-face of the sugar moiety, and also by the entropy of the system ($\Delta S°$).[4] The 2′-OH and 3′-OH drive the N⇌S pseudorotational equilibrium through the tendency to adopt a *gauche* arrangement of C-2′—O-2′ and C-3′—O-3′ bonds with C-1′—O-4′ and C-4′—O-4′ bonds, respectively. The heterocyclic base in *N*-nucleosides drives the two-state N⇌S pseudorotational equilibrium of the constituent β-D-pentofuranosyl moieties by the anomeric effect (i.e. electronic interaction between one of the lone-pair orbitals of O-4′ and the σ* orbital of the glycosidic bond), which places the aglycone in the pseudoaxial orientation (i.e. N-type conformation).[4]

Only a few studies have attempted to quantitate experimentally the activation energy of the furanose ring in nucleosides.[5–8] The analysis of the ^{13}C NMR relaxation measurements has shown that the average activation energy is 20 ± 2 kJ mol^{-1} for purine nucleosides.[5] Interpretation of longitudinal ^{13}C relaxation rates as a function of the reciprocal of temperature showed that the possible formation of an H-bond between 5′-OH and the base in liquid ammonia makes internal motions of pyrimidine nucleosides slow in comparison with rotational diffusion of the whole molecule. This supposed H-bonding interaction raised the apparent activation energies for uridine and cytosine nucleosides above 25 kJ mol^{-1}.[5]

^{13}C NMR relaxation parameters are often utilized in studies of dynamics because the relaxation of protonated carbons is dominated by dipolar interactions with the attached proton(s).[9] The analysis of temperature-dependent ^{13}C longitudinal relaxation times, however, suffers from the following limitations: (1) the C—H distances have to be known very accurately and (2) the dipolar interaction has to dominate T_1 relaxation of particular tertiary or secondary carbon on the pentofuranose moiety. On the other hand, deuterium is a quadrupole nucleus[10–19] and relaxes via a completely independent mechanism to ^{13}C, providing means of defining molecular dynamics without doubtful assumptions (e.g. bond distances from x-ray crystal structure are characterized with standard deviations around ±0.01 Å). Proton was specifically replaced by deuterium in a series of thymidine nucleosides **1**–**5a** and two abasic allofuranoses **6** and **7** (Scheme 1) in order to obtain an insight into their dynamic characteristics.

The stereochemical position of deuterium in different locations of nucleosides **1**–**5a** and sugars **6** and **7** is expected to be sensitive to the overall molecular reorientation and also to local internal motions such as a rapid interconversion between different pentofuranose puckering forms, reorientations of the nucleobase and 4-CH_2OH group. Deuterium in anh-6-DT (**5a**) is expected to monitor primarily the energy barrier for the overall molecular reorientation because rotation across χ and N⇌S repuckering are prevented by its structure. In this way, anh-6-DT (**5a**) will serve as a reference compound for the evaluation of activation energy of the overall tumbling also in the conformationally free counterparts **1**–**4**. Deuterium labels in **1**–**4** in comparison with **5a** undergo internal rotational motions that are coupled to the overall reorientation. We wish to evaluate individual contributions from the relative activation energy barriers of pseudorotation, rotation across χ and overall tumbling in pyrimidine nucleosides with the comparative analysis of temperature-dependent ^2H relaxation rates in **1**–**5**. The abasic allofuranoses **6** and **7** lack one rotational degree of freedom in comparison with **1**–**4** and therefore deuterium atoms bound to C-3 are expected to demonstrate how molecular motions change in the absence of heterocyclic base. The N⇌S pseudorotational equilibria in **6** and **7** are conformationally constrained by the fused isopropylidene moiety and are therefore expected to undergo very limited (if any) repuckering in comparison to nucleosides **1**–**4**.

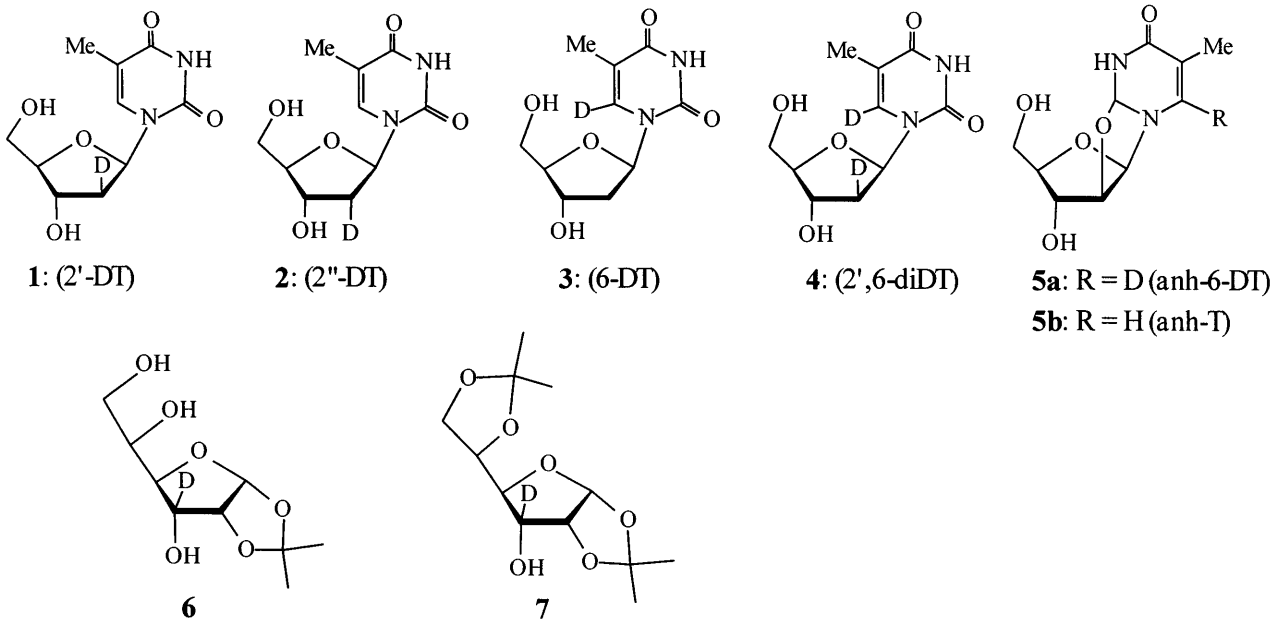

Scheme 1

RESULTS AND DISCUSSION

^{2}H and ^{13}C relaxation times

The deuterium and carbon spin–lattice relaxation times (T_1) were measured and analyzed in order to obtain an insight into molecular flexibility resulting from the rapid overall tumbling of nucleosides **1**–**5** and also internal conformational transitions including the interconversion between two low-energy N and S pseudorotamers. The observed relaxation rate is given in general by a reciprocal sum of the T_1 values from various contributing mechanisms such as dipole–dipole (T_1^{DD}), spin rotation (T_1^{SR}), chemical shift anisotropy (T_1^{CSA}), quadrupolar ($T_1{}^{Q}$) and other (T_1^{OTHER}) mechanisms:[9]

$$\frac{1}{T_1^{OBS}} = \frac{1}{T_1^{DD}} + \frac{1}{T_1^{SR}} + \frac{1}{T_1^{CSA}} + \frac{1}{T_1{}^{Q}} + \frac{1}{T_1^{OTHER}} \quad (1)$$

In the case of ^{2}H, the relaxation of which is dominated by the quadrupolar mechanism (i.e. $T_1{}^{Q}$), the spin–lattice relaxation time T_1 can be directly related to molecular motion.[9–19] The relationship between $T_1{}^{Q}$ and correlation time with the assumption of cylindrical symmetry of the electric field gradient tensor is given by

$$\frac{1}{T_1{}^{Q}} = \frac{3\pi^2}{2}\left(\frac{e^2qQ}{h}\right)^2 \tau_C \quad (2)$$

where (e^2qQ/h) is the quadrupole coupling constant and for sp^3 C—^{2}H bonds is in the range 130–200 kHz[10] and τ_C is the correlation time describing the reorientation of the relaxation vector. For nucleosides which undergo anisotropic motions τ_C should consist of components of motion about various axes and also internal motions. We did not attempt to extract all the rotational components from the relaxation data and the approximation was made that τ_C is replaced by an effective correlation time τ_{eff}. The experimental longitudinal (T_1) relaxation times for deuterium atoms in **1**–**7** were measured in the temperature range 278–358 k in 5 K steps (Tables 1 and 2). We also determined T_2 relaxation times and found that they are identical with T_1 values at a particular temperature, which proves that both nucleosides **1**–**5a** and sugars **6** and **7** undergo the motions in the extreme narrowing limit with $\omega\tau_c \ll 1$. The effective rotational correlation time (τ_{eff}) was calculated for **1**–**7** from deuterium T_1 with the use of Eqn (2) in the temperature range 278–358 K (Tables 1 and 2). At 278 K the overall molecular motion of **1**–**5a** is characterized by τ_{eff} in the range from 62.5 ps in **4** to 117.5 ps in **3**. The τ_{eff} values are reduced with the increase in temperature to 9.3 ps in **4** to 16 ps in **3** at 358 K (Table 1). The τ_{eff} values of **6** and **7** are 93.9 and 100.4 ps, respectively, at 278 K, which are reduced to 19.8 and 22.6 ps, respectively, at 328 K (Table 2). The comparison of T_1 relaxation times and τ_{eff} values in **1**–**5a** (Table 1) and sugars **6** and **7** (Table 2) shows that they are very similar at a particular temperature. It can be noted that molecular weights for **1**–**5a** and sugars **6** and **7** differ by only *ca.* 20 units, which suggests that their rotational tumblings are expected to be comparable. On the other hand, τ_{eff} is insensitive to the absence of heterocyclic

Table 1. Longitudinal deuterium T_1 relaxation times (ms) and effective correlation times (ps) for specifically sugar or nucleobase labelled thymidines **1**–**5a** as a function of temperature

	2′-DT (**1**) [D-2′]		2″-DT (**2**) [D-2″]		6-DT (**3**) [D-6]		2′,6-diDT (**4**) [D-6]]		2′,6-diDT (**4**) [D-2′]		anh-6-DT (**5a**) [D-6]	
T(K)	T_1	τ_{eff}	T_1	τ_{eff}	T_1	τ_{eff}	T_1	τ_{eff}	T_1	τ_{eff}	T_1	τ_{eff}
278	24.6	101.0	24.5	101.2	21.1	117.5	24.1	102.9	39.7	62.5	27.0	91.9
283	29.7	83.4	29.9	82.9	25.7	96.5	28.9	85.8	47.1	52.7		
288	37.2	66.6	38.5	64.4	31.0	80.0	37.2	66.7	50.6	49.0	43.1	57.5
293	44.3	56.0	44.4	55.9	36.9	67.2	46.7	53.1	68.0	36.5		
298	53.6	46.3	55.1	45.0	42.8	57.9	50.8	48.8	77.4	32.0	55.7	44.5
303	61.9	40.1	61.6	40.3	48.9	50.7	58.2	42.6	91.7	27.0		
308	70.6	35.1	72.3	34.3	56.2	44.1	68.3	36.3	92.9	26.7	78.0	31.8
313	82.5	30.1	81.9	30.3	63.6	39.0	71.5	34.7	103.4	24.0		
318	93.9	26.4	94.9	26.1	72.4	34.3	77.5	32.0	121.6	20.4	101.9	24.3
323	107.8	23.0	106.9	23.2	80.1	31.0	89.8	27.6	138.4	17.9		
328	122.0	20.3	121.5	20.4	91.4	27.1	106.4	23.3	151.7	16.3	111.6	22.2
333	133.8	18.5	136.0	18.2	101.4	24.5	117.0	21.2	172.5	14.4		
338	149.1	16.6	151.6	16.4	111.7	22.2	122.4	20.3	188.4	13.2	142.5	17.4
343	162.6	15.3	167.2	14.8	124.3	20.0	131.2	18.9	187.5	13.2		
348	179.6	13.8	186.6	13.3	133.8	18.5	145.3	17.1	231.4	10.7	175.3	14.1
353	199.2	12.4	201.0	12.3	144.8	17.1	171.7	14.4	241.5	10.3		
358	216.5	11.5	220.5	11.2	156.5	15.8	183.3	13.5	268.1	9.3	191.5	13.0

[a] The spin–lattice relaxation time T_1 (±10%) was calculated by using intensity and area fits, which showed deviation of *ca.* 5%. τ_{eff} was calculated with the use of Eqn (2) with a deuterium quadrupole coupling constant (e^2qQ/h) of 165 kHz.

Table 2. Longitudinal deuterium T_1 relaxation times (ms) and effective correlation times (ps) for specifically deuterated **6** and **7** as a function of temperature

	6		**7**	
T(K)	T_1	τ_{eff}	T_1	τ_{eff}
278	26.4	93.9	24.7	100.4
288	39.7	62.5	36.1	68.7
298	56.2	44.1	50.0	49.6
308	77.1	32.2	66.2	37.5
318	99.0	25.1	88.7	28.0
328	125.5	19.8	109.6	22.6
338	155.1	16.0	—	—

[a] T_1 ($\pm$10%) and τ_{eff} are given in units of ms and ps, respectively. τ_{eff} was calculated with the use of Eqn (2) with an e^2qQ/h of 165 kHz.

aglycone in **6** and **7** in comparison with **1**–**5a**.

The relaxation of ^{13}C, which is the most common nucleus in studies of molecular dynamics by NMR, is dominated by dipolar interactions with bonded protons (T_1^{DD}).[9] The T_1 dipole–dipole ^{13}C relaxation time is under the extreme narrowing conditions ($\omega\tau_C \ll 1$) interpreted by the equation

$$\frac{1}{T_1^{DD}} = \frac{N\gamma_C{}^2\gamma_H{}^2h^2}{4\pi^2r_{CH}^6}\tau_{eff} \quad (3)$$

where N is the number of attached hydrogens and r_{CH} is the C—H bond distance. Longitudinal ^{13}C relaxation times were collected as a function of temperature in the range 278–358 K for 2′-DT (**1**, Table 3) and anh-T (**5b**, Table 4). It is evident that the T_1 values in 2′-DT (**1**) at 278 K are very similar for the sugar carbon atoms C-1′, C-3′ and C-4′ and also C-6 within the limits of experimental error. In the case of C-5′ the relaxation time data become comparable when we take into account that it is a secondary carbon and therefore two protons participate in dipole interactions which determine T_1 [Eqn (3)]. The effective rotational correlation time in 2′-DT (1) and anh-T (**5b**) was calculated from T_1 of ^{13}C with the use of Eqn (3) in the temperature range 278–358 K (Tables 3 and 4, respectively). The overall molecular motion of 2′-DT (**1**) at 278 K is characterized by τ_{eff} in the range from 89.8 ps (C-3′) to 122.2 ps (C-4′), and is reduced to values in the range from 9.5 ps (C-3′)

Table 3. ^{13}C longitudinal (T_1) relaxation times (s) of secondary and tertiary carbon atoms and effective correlation times (ps) as a function of temperature for 2-DT (**1**)

	[C-1′]		[C-2′]	[C-3′]		[C-4′]		[C-5′]		[C-6]	
T (K)	T_1	τ_{eff}	T_1	T_1	τ_{eff}	T_1	τ_{eff}	T_1	τ_{eff}	T_1	τ_{eff}
278	0.38	115.8	0.48	0.49	89.8	0.36	122.2	0.20	110.0	0.36	109.2
283	0.64	68.7	0.71	0.76	57.9	0.57	77.2	0.32	68.7	0.40	98.3
288	0.73	60.3	0.83	1.02	43.1	0.64	68.7	0.36	61.1	0.63	62.4
293	0.87	50.6	1.02	1.18	37.3	0.75	58.7	0.41	53.6	0.75	52.4
298	0.94	46.8	1.10	1.44	30.5	0.99	44.4	0.48	45.8	0.87	45.2
303	1.23	35.8	1.56	1.67	26.3	1.07	41.1	0.64	34.4	0.91	43.2
308	1.35	32.6	1.58	1.84	23.9	1.21	36.4	0.63	34.9	1.14	34.5
313	1.42	31.0	1.67	2.03	21.7	1.40	31.4	0.81	27.2	1.21	32.5
318	1.82	24.2	2.17	2.53	17.4	1.67	26.3	0.89	24.7	1.23	32.0
328	2.08	21.1	3.02	2.92	15.1	1.96	22.4	1.02	21.6	1.66	23.7
338	2.56	17.2	2.96	3.95	11.1	2.39	18.4	1.54	14.3	2.15	18.3
348	3.25	13.5	4.03	4.62	9.5	2.89	15.2	1.87	11.8	3.01	13.1

[a] T_1 ($\pm$10%) and τ_{eff} are given in units of s and ps, respectively. τ_{eff} was calculated with the use of Eqn (3) with a bond distance d_{C-H} of 1.08 Å, except for $d_{C\text{-}6\text{–}H\text{-}6}$ = 1.06 Å[4c].

Table 4. ^{13}C longitudinal (T_1) relaxation times (s) of secondary and tertiary carbon atoms and effective correlation times (ps) as a function of temperature for anh-T (**5b**)

	[C-1′]		[C-2′]		[C-3′]		[C-4′]		[C-5′]		[C-6]	
T (K)	T_1	τ_{eff}	T_1	τ_{eff}	T_1	τ_{eff}	T_1	τ_{eff}	T_1	τ_{eff}	T_1	τ_{eff}
283	0.55	80.0	0.47	93.6	0.54	81.5	0.47	93.6	0.24	91.6	0.41	95.9
308	1.15	38.3	0.97	45.4	1.19	37.0	1.05	41.9	0.60	36.7	1.07	36.8
333	1.88	23.4	1.89	23.3	2.50	17.6	1.89	23.3	1.27	17.3	2.03	19.4
358	—	—	2.37	18.6	4.62	9.5	2.37	18.6	1.58	13.9	3.56	11.0

[a] T_1 ($\pm$10%) and τ_{eff} are given in units of s and ps, respectively. τ_{eff} was calculated with the use of Eqn (3) with a bond distance d_{C-H} of 1.08 Å, except for $d_{C\text{-}6\text{–}H\text{-}6}$ = 1.06 Å[4C].

to 15.2 ps (C-4′, see Table 3) at 348 K. In the case of anh-T (**5b**), the molecular motion is characterized by τ_{eff} in the range from 80.0 ps (C-1′) to 95.9 ps (C-6) at 283 K (Table 4). The estimates of τ_{eff} for anh-T (**5b**) are reduced with increase in temperature to values in the range from 9.5 s (C-3′) to 18.6 ps (C-2′ and C-4′) at 358 K (Table 4).

Deuterium quadrupole coupling constant

The comparison of the corresponding ^{2}H and ^{13}C relaxation times in 2′-DT (**1**) enabled us to calculate the deuterium quadrupole coupling constant.[16,17,19] The effective correlation time (τ_{eff}) from deuterium relaxation [eqn (2)] describes the reorientation of the C—^{2}H vector and can be directly compared with τ_{eff} from ^{13}C dipole–dipole relaxation [Eqn (3)], which is dependent on the reorientation of the ^{13}C–^{1}H vector. The C–H bond distance was estimated to be 1.08 Å based on *ab initio* calculations at the HF/3–21G level.[4a,c] Twelve T_1 values of D-2′ and carbon atoms in 2′-DT (**1**) at various temperatures in the range 278–348 K (see Tables 1 and 3) were used in the calculation of the deuterium quadrupole coupling constant (e^2qQ/h). The results showed that (i) the estimates from C-1′ (168) kHz, C-4′ (161 kHz) and C-5′ (171 kHz) are very similar and the average calculated deuterium quadrupole coupling constant is 167 kHz and (ii) the calculations with C-2′ (185 kHz) and C-3′ (198 kHz) gave higher values of quadrupole coupling constant which could indicate alternative relaxation pathways to ^{13}C relaxation other than dipolar contribution for these two carbons in 2′-DT (**1**).

Temperature dependence of longitudinal relaxation times

The experimental longitudinal (T_1) relaxation time for deuterium atoms in **1**–**7** which were obtained at various temperatures in the range 278–358 K are given in Tables 1 and 2. These data show slight variations of T_1 relaxation times with the structures of **1**–**7**, whereas their temperature dependences are nearly identical. The temperature dependence of T_1 was evaluated with the use of an Arrhenius-type equation and we observed that the straight lines for D-2′, D-2″ and D-6 in **1**–**5a** are almost parallel (Fig. 1). The slopes of the best-fit lines shown in Fig. 1 are directly related to the apparent activation energy. The estimates of E_a were found to be in the range 20–22 kJ mol^{-1} (Table 5). The temperature dependence of T_1 in **6** and **7** [Fig. 1(B)] gave apparent E_a values of 22.9 and 22.7 kJ mol^{-1}, respectively (Table 5). The E_a values show that the comparison of the relaxation data of deuterium atoms bound to different parts of the molecule in **1**–**5a**, which are undergoing reorientation across χ and N⇌S repuckering of the deoxyribose moiety, does not allow dissection of the two contributions to the internal motion from the overall molecular tumbling. The macroscopic viscosity of the pure water changes in the temperature range of our study from 1.5×10^{-3} at 278 K to 0.3×10^{-3} kg m^{-1} s^{-1} at 358 K. Deuterium T_1 relaxation times of **1**–**7** showed no concentration dependence in the range 16–247 mM, which indicates that the effect of association of the solute on the correlation times for the overall molecular tumbling and internal dynamics of the sugar moiety is negligible. Decreased hydrogen bonding of the solute molecules with water at elevated temperature is expected to increase the quadrupole coupling constant and decrease the correlation time,[10] which should cancel in their effect on T_1 values [Eqn (2)]. Despite the fact that the polarities of **1**–**7** are not equivalent, their temperature-dependent experimental T_1 relaxation times are nearly identical within the experimental error; hence temperature-dependent changes in solvent viscosity and the viscosity correction of the relaxation times have little effect on intramolecular energy barriers.[15,20] It is noteworthy that removal of the nucleobase in **6** and **7** gives comparable E_a values, thus showing their insensitivity to the absence of heterocyclic aglycone in **6** and **7** in comparison with **1**–**5a**.

Table 5. Apparent activation energies of **1**–**7** in H_2O obtained from semi-logarithmic plots of deuterium T_1 relaxation time as a function of reciprocal of temperature

Compound	Atom	E_a (kJ mol^{-1})[a]
2′-DT (**1**)	[D-2′]	22.3 (±0.4)
2″-DT (**2**)	[D-2″]	22.4 (±0.4)
6-DT (**3**)	[D-6]	20.5 (±0.3)
2′,6-diDT (**4**)	[D-2′]	20.2 (±0.3)
2′,6-diDT (**4**)	[D-6]	20.0 (±0.3)
anh-6-DT (**5a**)	[D-6]	20.0 (±0.9)
6	[D-3′]	22.9 (±0.9)
7	[D-3′]	22.7 (±0.9)

[a] Calculated from the slopes of straight lines shown in Fig. 1 according to the relationship $T_1 = (T_1)_0 \exp(-E_a/RT)$.

The fact that sugar **7** is conformationally constrained, as is the sugar moiety in anh-6-DT (**5a**), and they have comparable E_a values to the corresponding non-constrained counterparts **6** and 6-DT (**3**), respectively, suggests that no contribution to the observed E_a in these compounds comes from the energy of activation necessary for the interconversions between envelope and twist forms of five-membered rings. Note that the pair of 6-DT (**3**) and anh-6-DT (**5a**) have comparable E_a and therefore the observed E_as cannot be separated into the contributions from overall and internal molecular motions.

Longitudinal ^{13}C relaxation times were measured as a function of temperature in the range 278–358 K for 2′-DT (**1**) and anh-T (**5b**). The plot of lnT_1 as a function of 1000/T in Fig. 2 shows that there is no difference between the relaxation behaviour of C-6, sugar carbon atoms or C-5′ in 2′-DT (**1**, panel A) or anh-T (**5b**, panel B) and the straight lines through the experimental data points are parallel. The slopes of the straight lines in

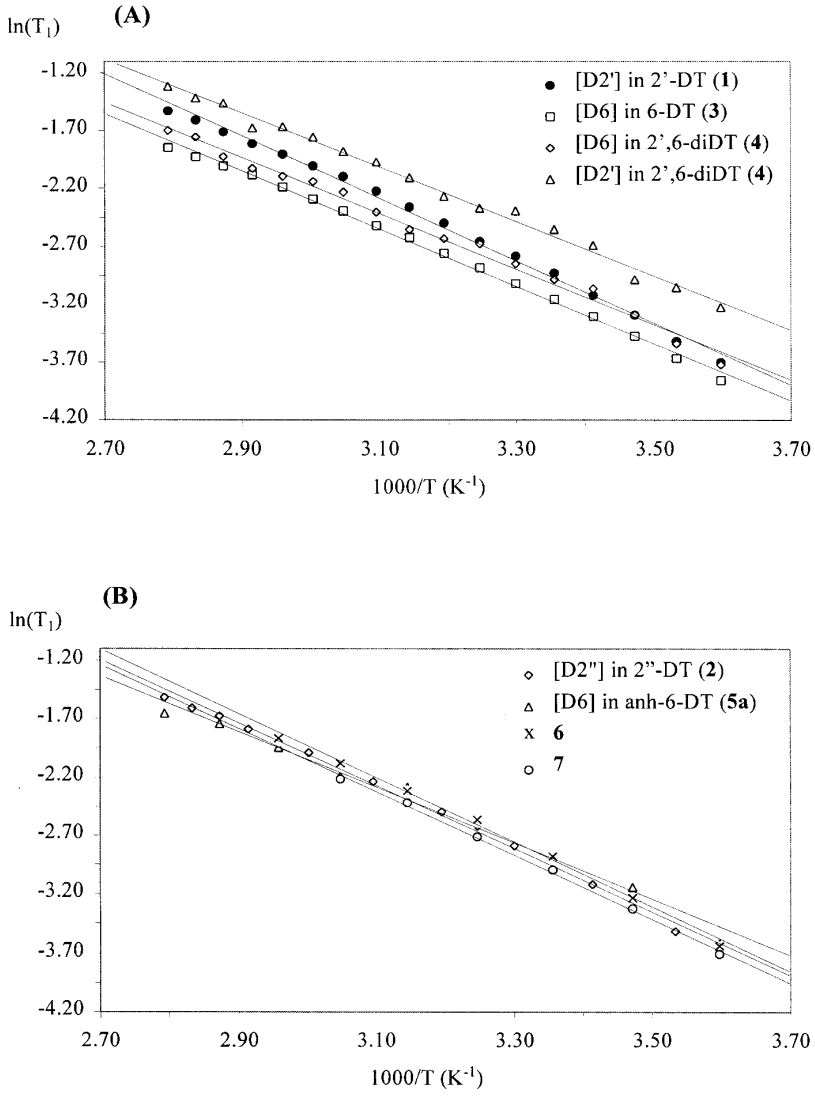

Figure 1. Longitudinal deuterium relaxation time as a function of reciprocal of temperature. Straight lines in (A) were obtained by linear regression and are characterized by the slope of -2.68 ($\sigma = 0.05$) and intercept of 6.0 ($\sigma = 0.2$) for 2′-DT (**1**), the slope of -2.47 ($\sigma = 0.04$) and intercept of 5.1 ($\sigma = 0.1$) for 6-DT (**3**), the slope of -2.43 ($\sigma = 0.04$) and intercept of 5.1 ($\sigma = 0.1$) for [D-6] and the slope of -2.41 ($\sigma = 0.04$) and intercept of 5.4 ($\sigma = 0.1$) for [D-2′] in 2′,6-diDT (**4**). Straight lines in (B) were obtained by linear regression and are characterized by the slope of -2.70 ($\sigma = 0.05$) and intercept of 6.1 ($\sigma = 0.1$) for 2″-DT (**2**), the slope of -2.40 ($\sigma = 0.1$) and intercept of 5.1 ($\sigma = 0.3$) for anh-6-DT (**5a**), the slope of -2.76 ($\sigma = 0.1$) and intercept of 6.35 ($\sigma = 0.3$) for **6** and the slope of -2.73 ($\sigma = 0.2$) and intercept of 6.13 ($\sigma = 0.2$) for **7**.

Fig. 2 for each carbon in 2′-DT (**1**) and anh-T (**5b**) gave estimates of apparent E_a (Table 6). The average E_a values from the six estimates for 2′DT (**1**) and anh-T (**5b**) in Table 6 are 23.1 and 21.1 kJ mol^{-1} respectively. The difference of 2 kJ mol^{-1} is of the order of the experimental error and does not enable us to dissect individual intramolecular motions from the overall tumbling.

The deuterium atoms in 2′-DT (**1**) and 2″-DT (**2** are in chemically and magnetically non-equivalent positions. However, the relaxation of C-2—D2′ and C-2′—D2″ vectors shows very similar behaviour. This could possibly indicate that the pseudorotational energy barrier is very small. On the other hand, the overall tumbling of selectively deuterated thymidines **1**–**5a** might be characterized by the frequency that is compa-

Table 6. Apparent activation energies (kJ mol^{-1}) of 2′-DT (**1**) and anh-T (**5b**) in D_2O obtained from semi-logarithmic plots of ^{13}C T_1 relaxation time as a function of reciprocal of temperature

Compound	[C-1′]	[C-2′]	[C-3′]	[C-4′]	[C-5′]	[C-6]
2′-DT (**1**)	22.4 (±2)	23.3 (±2)	24.1 (±1)	22.4 (±1)	24.1 (±1)	22.4 (±1)
anh-T (**5b**)	19.1 (±2)	19.1 (±2)	24.1 (±1)	18.3 (±3)	21.6 (±3)	24.1 (±1)

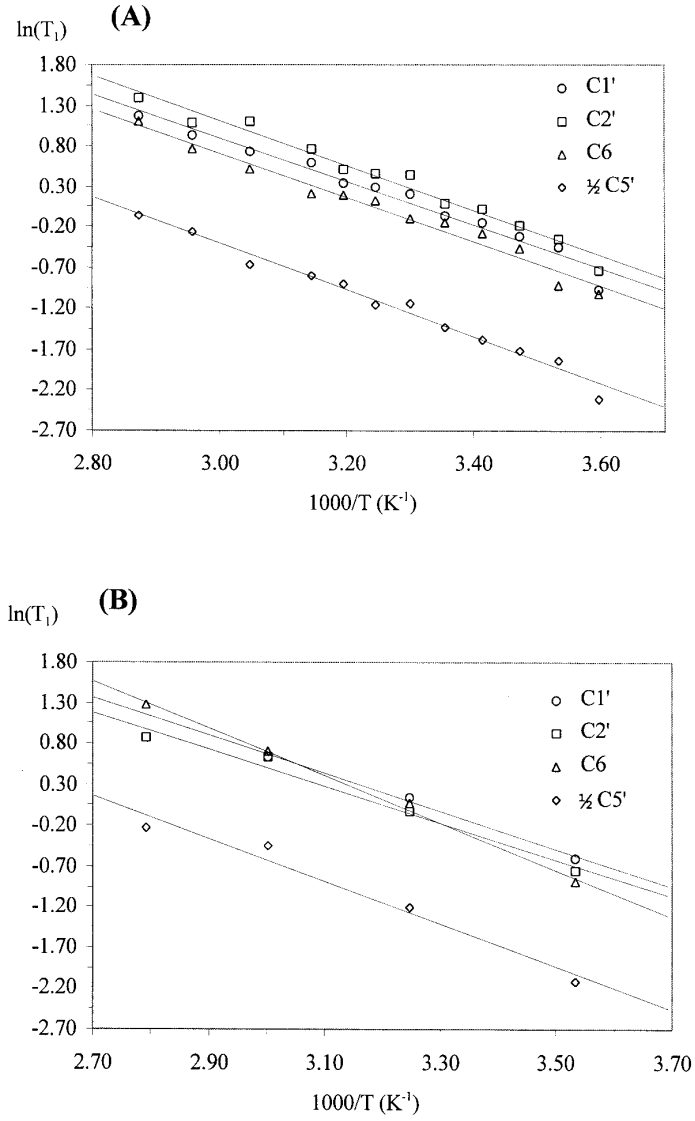

Figure 2. Longitudinal ^{13}C relaxation times as a function of reciprocal of temperature for (A) 2′-DT (**1**) and (B) anh-T (**5b**). For clarity only selected temperature-dependent T_1 values are shown for C-1′ (○), C-2′ (□), C-6 (△) and C-5′ (◇) in both panels. Straight lines were obtained by linear regression and are characterized by the slope of -2.7 ($\sigma = 0.2$) and intercept of 8.9 ($\sigma = 0.5$) for C-1′, the slope of -2.8 ($\sigma = 0.2$) and intercept of 9.5 ($\sigma = 0.5$) for C-2′, the slope of -2.9 ($\sigma = 0.2$) and intercept of 9.9 ($\sigma = 0.5$) for C-3′, the slope of -2.7 ($\sigma = 0.1$) and intercept of 8.9 ($\sigma = 0.4$) for C-4′, the slope of -2.7 ($\sigma = 0.1$) and intercept of 8.9 ($\sigma = 0.5$) for C-6 and the slope of -2.9 ($\sigma = 0.1$) and intercept of 8.2 ($\sigma = 0.4$) for C-5′ in 2′-DT (**1**) and the slope of -2.3 ($\sigma = 0.2$) and intercept of 7.6 ($\sigma = 0.5$) for C-1′, the slope of -2.3 ($\sigma = 0.2$) and intercept of 7.3 ($\sigma = 0.8$) for C-2′, the slope of -2.9 ($\sigma = 0.1$) and intercept of 9.7 ($\sigma = 0.1$) for C-3′, the slope of -2.2 ($\sigma = 0.3$) and intercept of 7.2 ($\sigma = 0.8$) for C-4′, the slope of -2.9 ($\sigma = 0.1$) and intercept of 9.4 ($\sigma = 0.4$) for C-6′ and the slope of -2.6 ($\sigma = 0.3$) and intercept of 7.3 ($\sigma = 1.1$) for C-5′ in anh-T (**5b**).

rable to N to S re-puckering, which would mean that these two (and possibly other) dynamic events are heavily mixed. In such a case, the separation of the overall tumbling, rotation across glycosyl bond as monitored through relaxation of the C-6—D-6 vector and conformational interconversions on the pseudorotational cycle are not possible.

Several *ab initio* calculations on nucleosides at various levels of theory showed two energy wells in the N and S regions of pseudorotational space.[4,21] In addition, the pseudorotational energy profiles[4a,c,21] showed energy barriers in the east region of conformational space between 14.9 and 24.0 kJ mol^{-1}, which suggests a rapid exchange on the NMR time-scale between interconverting conformers.

CONCLUSIONS

Specifically deuterated thymidines **1**–**5a** and two C-3 deuterated allofuranoses **6** and **7** served as model compounds with selective probes to define molecular motions through deuterium relaxation. Deuterium relaxation times in **1**–**5a** were found in the range 20–270 ms between 278 and 358 K, respectively. Interpretation

of the deuterium T_1 relaxation time, which is dominated by a quadrupole mechanism, gave the effective rotational correlation time (τ_{eff}) in the range from 62.5 ps in 2,6-diDT (**4**) to 117.5 ps in 6-DT (**3**) at 278 K. The τ_{eff} values are reduced with increase in temperature to values in the range from 9.3 ps in 2′,6-diDT (**4**) to 16 ps in 6-DT (**3**) at 358 K. The τ_{eff} values for **6** and **7** are 93.9 and 100.4 ps, respectively, at 278 K, and are reduced to 19.8 and 22.6, respectively, at 328 K. The comparison of the experimental T_1 relaxation times and calculated τ_{eff} values for **1–5a** with those from abasic sugars **6** and **7** shows close similarity at a particular temperature and allows no dissection into specific local intramolecular motions.

Through the comparison of ^{2}H and ^{13}C relaxation times in 2′-DT (**1**) we calculated the deuterium quadrupole coupling constant (e^2qQ/h) to be 167 kHz.

The temperature dependence of deuterium T_1 relaxation times in **1–7** gave apparent activation energies in the range 20–23 kJ mol^{-1}. Deuterium in anh-6-DT (**5a**) gave an estimate of the energy barrier (20.0 $\pm$ 0.9 kJ mol^{-1}) for the overall molecular reorientation because it cannot undergo internal rotations across χ and N$\rightleftharpoons$S repuckering. However, the deuterium labels in **1–4** in comparison with **5a** undergo internal rotational motions that are heavily coupled to their overall reorientation, which prevents dissection of individual experimental E_a values into the contributions from activation energy barriers is pseudo-rotation, rotation across χ and overall tumbling. The apparent activation energy is insensitive to the absence of the heterocyclic base in abasic sugars **6** and **7**. The comparison of the conformational dynamics of conformationally free nucleosides **1–4** with the corresponding constrained analogue **5a** and abasic **6** and **7** showed limitations of the analysis of temperature-dependent deuterium T_1 relaxation times in the study of pseudo-rotation energy barriers. Strong dynamic coupling of local motions in **1–7** prevents the dissection and correlation of the structural effects with the overall reorientation, internal rotations across χ and γ or pentofuranose repuckering.

EXPERIMENTAL

The ^{2}H and ^{13}C NMR spectra were recorded at 76.77 and 125.74 MHz, respectively, on a Bruker AMX 500 NMR spectrometer at a magnetic field of 11.7 T. All deuterium spectra were acquired in H_2O at 17 temperatures between 278 and 358 K in 5 K steps at neutral pH and 0.2 M concentration. The minor concentration dependence of T_1 and T_2 relaxation times in the range 16–247 mM was within the limits of experimental error ($\pm$10%). Each of the compounds was lyophilized from H_2O three times prior to T_1 and T_2 measurements, which reduced the solvent signal to *ca.* 50% of the signals from the compounds. All samples were degassed prior to relaxation time measurements. The sample temperature was controlled to within *ca.* $\pm$0.5 K. Trifluoroethanol (8 µl) was used for ^{19}F lock. The ^{2}H NMR measurements were performed under the following spectral and processing conditions: 2100 Hz spectral width, 13.5 µs (90°) pulse length, a pulse delay of 1 s, 64 scans, 16 K time domain and line broadening of 1 Hz prior to Fourier transformation. All T_1 experiments were carried out using the inversion–recovery technique, whereas T_2 was determined with the use of the CPMG sequence. Pulse lengths of 90° and 180° were measured prior to recording each data set. Twelve relaxation delays were utilized in the experiments for the determination of T_1 and T_2. The fits of area and intensity of a particular signal were averaged to obtain the relaxation times at each temperature (the deviation was below 5%). T_1 and T_2 values for ^{2}H and ^{13}C were calculated with the aid of Bruker software.

Acknowledgements

We thank the Swedish Natural Science Research (NFR) Council, the Swedish Technical Research Council (TFR) and the Ministry of Science and Technology of the Republic of Slovenia for generous financial support. Thanks are due to the Wallenbergstiftelsen, Forskningsrådsnämnden and the University of Uppsala for funds for the purchase of 500 and 600 MHz Bruker DRX NMR spectrometers.

REFERENCES

1. W. Saenger, *Principles of Nucleic Acid Structure.* Springer, Berlin (1988).
2. C. Altona, and M. Sundaralingam, *J. Am. Chem. Soc.* **94**, 8205 (1972); **95**, 2333 (1973).
3. (a) J. Feigon, A. H.-J. Wang, G. A. van der Marel, J. H. van Boom and A. Rich, *Nucleic Acids Res.* **12**, 1243 (1984); (b) S. Tran-Dinh, J. Taboury, J.-M. Neumann, T. Huynh-Dinh, B. Genissel, B. Laglois d'Estaintot and J. Igolen, *Biochemistry* **23**, 1362 (1984); (c) P. W. Davis, K. Hall, P. Cruz, I. Tinoco and T. Neilson, *Nucleic Acids Res.* **14**, 1279 (1986); (d) P. W. Davis, R. W. Adamiak and I. Tinoco, *Biopolymers* **29**, 109 (1990); (e) P. Agback, A. Sandstrom, S.-I. Yamakage, C. Sund, C. Glemarec and J. Chattopadhyaya, *J. Biochem. Biophys. Methods* **27**, 229 (1993); (f) P. Agback, C. Glemarec, L. Yin, A. Sandstrom, J. Plavec, C. Sund, S.-I. Yamakage, G. Wiswanadham, B. Rousse, N. Puri and J. Chattopadhyaya, *Tetrahedron Lett.* **34**, 3929 (1993).
4. (a) J. Plavec, W. Tong and J. Chattopadhyaya, *J. Am. Chem. Soc.* **115**, 9734 (1993); (b) J. Plavec, N. Garg and J. Chattopadhyaya, *J. Chem. Soc., Chem. Commun.* 1011 (1993); (c) J. Plavec, L. H. Koole and J. Chattopadhyaya, *J. Biochem. Biophys. Methods* **25**, 253 (1992); (d) L. H. Koole, H. M. Buck, A. Nyilas and J. Chattopadhyaya, *Can J. Chem.* **65**, 2089 (1987); (e) L. H. Koole, H. M. Buck, H. Bazin and J. Chattopadhyaya, *Tetrahedron* **43**, 2289 (1987); (f) L. H. Koole, J. Plavec, H. Liu, B. R. Vincent, M. R. Dyson, P. L. Coe, R. T. Walker, G. W. Hardy, S. G. Rahim and J. Chattopadhyaya, *J. Am. Chem. Soc.* **114**, 9934 (1992); (g) J. Plavec, C. Thibaudeau, G. Viswanadham, C. Sund and J. Chattopadyaya, *J. Chem. Soc., Chem. Commun.* 781 (1994); (h) C. Thibaudeau, J. Plavec, K. A. Watanabe and J. Chattopadhyaya, *J. Chem. Soc., Chem. Commun* 537 (1994); (i) C. Thibaudeau, J. Plavec, N. Garg, A. Papchikhin and J. Chattopadhyaya, *J. Am. Chem. Soc.* **116**, 4038 (1994); (j) J. Plavec, C. Thibaudeau and J. Chattopadhyaya, *J. Am. Chem. Soc.* **116**, 6558 (1994); (k) C. Thibaudeau, J. Plavec and J. Chattopadhyaya, *J. Am. Chem. Soc.* **116**, 8033 (1994); (l) J. Plavec, PhD Thesis, Uppsala University (1995); (m) J. Plavec, C. Thibaudeau and J. Chattopadhyaya, *Tetrahedron* **51**, 11775 (1995); (n) C. Thibeaudeau, J. Plavec, and J. Chattopadhyaya, *J. Org. Chem.* **61** 266 (1996); (o) J. Chattopadhyaya, *Nucleic Acids Symp. Ser.* **35**, 111 (1996); (p) J. Plavec, C. Thibaudeau and J. Chattopadhyaya, *Pure Appl. Chem.* **68**, 2137 (1996); (r) I. Luyten, C. Thibaudeau and J. Chattopadhyaya, *Tetrahedron* **53**, 6433 (1997); (s) I. Luyten, C. Thibaudeau and J. Chattopadhyaya, *Tetrahedron* **53**, 6903 (1997); (t) I. Luyten, C. Thibaudeau and J. Chattopadhyaya, *J. Org. Chem.* **62**, 8800 (1997); (u) C. Thibau-

deau, A. Földesi and J. Chattopadhyaya, *Tetrehedron* **53**, 14043 (1997).
5. O. Röder, H.-D. Lüdermann and E. von. Goldammer, *Eur, J. Biochem.* **53**, 517 (1975).
6. L. M. Rhodes and P. R. Schimmel, *Biochemistry* **10**, 4426 (1971).
7. H.-D. Lüdemann, O. Roder, E. Westhof, E. v. Goldammer and A. Muller, *Biophys. Struct. Mech.* **1**, 121 (1975).
8. H.-D. Lüdeman and E. Westhof, in *Nuclear Magnetic Resonance in Molecular Biology* edited by B. Pullman, p. 41. Reidel, Dordrecht (1978).
9. J. Sandström, *Dynamic NMR Spectroscopy*. Academic Press, London (1982).
10. H. H. Mantsch, H. Saito and I. C. P. Smith, *Prog. Nucl. Magn. Reson. Spectrosc.* **11**, 211 (1977).
11. R. G. Kidd, in *NMR of Newly Accessible Nuclei*, edited by P. Laszlo, Vol. 1, p. 103. Academic Press, New York (1983).
12. H. C. Jarrell, I. C. P. Smith, in *Applications of High Resolution Deuterium Magnetic Resonance, NATO ASI Series C103*, edited by J. B. Lambert and F. G. Riddell, p. 133. Reidel, Dordrecht (1983).
13. S. Schramm and E. Oldfield, *Biochemistry* **22**, 2908 (1983).
14. I. C. P. Smith, and H H. Mantsch, *ACS Symp. Ser.* **191**, 97 (1982).
15. W. Egan, *J. Am. Chem. Soc.* **98**, 4091 (1976).
16. A. P. Zens, P. T. Fogle, T. A. Bryson, R. B. Dunlap, R. R. Fisher and P. D. Ellis, *J. Am. Chem. Soc.* **98**, 3760 (1976).
17. A. P. Zens, T. A. Bryson, R. B. Dunlap, R. R. Fisher and P. D. Ellis, *J. Am. Chem. Soc.* **98**, 7559 (1976).
18. C. Brevard, J. P. Kintzinger and J. M. Lehn, *J. Chem. Soc., Chem. Commun.* 1193 (1969).
19. H. Saito, H. H. Mantsch and I. C. P. Smith, *J. Am. Chem. Soc.* **95**, 8453 (1973).
20. H.-D. Lüdemann and O. Röder, *J. Am. Chem. Soc.* **97**, 4402 (1975).
21. M. Polak, B. Mohar, J. Kobe and J. Plavec, *J. Am. Chem. Soc.* **120**, 2508 (1998).

